



Article

Micheliolide Enhances Radiosensitivities of p53-Deficient Non-Small-Cell Lung Cancer via Promoting HIF-1 α Degradation

Peizhong Kong^{1,2}, K.N. Yu^{3,4}, Miaomiao Yang^{1,2}, Waleed Abdelbagi Almahi^{1,2}, Lili Nie¹, Guodong Chen^{1,*} and Wei Han^{1,5,*}

¹ Anhui Province Key Laboratory of Medical Physics and Technology/Center of Medical Physics and Technology, Hefei Institutes of Physical Sciences, Chinese Academy of Sciences, Hefei 230031, China; gckongpz@163.com (P.K.); yangmiaomiaom@163.com (M.Y.); wdsudanese@yahoo.com (W.A.A.); niell@cmpt.ac.cn (L.N.)

² Science Island Branch of Graduate School, University of Science and Technology of China, Hefei 230026, China

³ Department of Physics, City University of Hong Kong, Tat Chee Avenue, Kowloon Tong 999077, Hong Kong; peter.yu@cityu.edu.hk

⁴ State Key Laboratory in Marine Pollution, City University of Hong Kong, Tat Chee Avenue, Kowloon Tong 999077, Hong Kong

⁵ Collaborative Innovation Center of Radiation Medicine of Jiangsu Higher Education Institutions and School for Radiological and Interdisciplinary Sciences (RAD-X), Soochow University, Suzhou 215123, China

* Correspondence: c3024034@163.com (G.C.); hanw@hfcas.ac.cn (W.H.); Tel.: +86-551-65595385 (G.C.); +86-511-65595100 (W.H.)

Received: 30 April 2020; Accepted: 8 May 2020; Published: 11 May 2020



Abstract: Micheliolide (MCL) has shown promising anti-inflammatory and anti-tumor efficacy. However, whether and how MCL enhances the sensitivity of non-small-cell lung cancer (NSCLC) to radiotherapy are still unknown. In the present paper, we found that MCL exerted a tumor cell killing effect on NSCLC cells in a dose-dependent manner, and MCL strongly sensitized p53-deficient NSCLC cells, but not the cells with wild-type p53 to irradiation (IR). Meanwhile, MCL markedly inhibited the expression of hypoxia-inducible factor-1 α (HIF-1 α) after IR and hypoxic exposure in H1299 and Calu-1 cells rather than in H460 cells. Consistently, radiation- or hypoxia-induced expression of vascular endothelial growth factor (VEGF) was also significantly inhibited by MCL in H1299 and Calu-1 cells, but not in H460 cells. Therefore, inhibition of the HIF-1 α pathway might, at least in part, contribute to the radiosensitizing effect of MCL. Further study showed that MCL could accelerate the degradation of HIF-1 α through the ubiquitin-proteasome system. In addition, the transfection of wild-type p53 into p53-null cells (H1299) attenuated the effect of MCL on inhibiting HIF-1 α expression. These results suggest MCL effectively sensitizes p53-deficient NSCLC cells to IR in a manner of inhibiting the HIF-1 α pathway via promoting HIF-1 α degradation, and p53 played a negative role in MCL-induced HIF-1 α degradation.

Keywords: micheliolide; radiosensitizer; hypoxia-inducible factor-1 α ; vascular endothelial growth factor; p53

1. Introduction

Lung cancer is the leading cause of cancer incidence and mortality worldwide, and non-small-cell lung cancer (NSCLC) is the most common histological subtype of lung cancers [1,2]. Radiotherapy is widely used, due to its advantages for NSCLC patients, especially in cases where the tumour is

unresectable or the patient is inoperable [3]. However, radioresistance still remains a main obstacle limiting the efficacy of radiotherapy. Extensive efforts have been made to understand the mechanisms underlying radioresistance. The factors that are involved in the development of radioresistance include enhanced DNA damage repair, tumor metabolism alteration, cell cycle redistribution, as well as changes in the tumor microenvironment [4]. In particular, hypoxia, a general hallmark of tumor microenvironment, has been reported to be associated with radioresistance and hypoxia-inducible factor-1 (HIF-1) plays a major role in hypoxia-related radioresistance [5,6].

HIF-1 is a heterodimer that is composed of a regulatory HIF-1 α subunit and a constitutively expressed HIF-1 β subunit [7]. As an oxygen-dependent transcriptional factor, HIF-1 is increased and it promotes the transcription of genes associated with angiogenesis, cell survival, glucose metabolism, and invasion under hypoxic conditions in cancer cells. The change of HIF-1 α protein level in response to normoxia/hypoxia mainly depends on the regulation of HIF-1 α degradation. Under normoxic conditions, HIF-1 α is hydroxylated and then ubiquitinated, which leads to a rapid degradation with a half-life of 5–8 min [8,9]. On the contrary, the degradation of HIF-1 α could be inhibited by hypoxia, resulting in the accumulation of HIF-1 α . Except hypoxia, oxidative stress and oncogenes also promote the activity of HIF-1 [10–12]. Previous researches have shown that radiation could increase the level of HIF-1 α protein in a subset of radioresistant lung cancer cell lines [13]. The mechanism study revealed that the activation of phosphatidylinositol 3-kinase (PI3K)/Akt/mTOR increases de novo protein synthesis of HIF-1 α and enhanced the interaction between heat shock protein 90 (Hsp90) and HIF-1 α after irradiation (IR) [13].

Elevated HIF-1 α protein expression promoted the secretion of vascular endothelial growth factor (VEGF), which mediated tumor-protective response to radiotherapy via vascular protection or inhibiting IR-induced apoptosis by upregulating anti-apoptosis protein, Bcl-2 [13–15]. In addition, hypoxia-induced HIF-1 α activated the expression of glucose transporter-1 (GLUT-1), which conferred the enhanced tumor antioxidant capacity linking to radioresistance through initiating a glycolytic tumor metabolism [16]. Consistently, a number of clinical studies have also confirmed that HIF-1 α overexpression has tight association with the poor prognosis to radiotherapy in various cancer types [17–19]. Therefore, HIF-1 is a target of sensitization for cancer radiotherapy, and many HIF-1 α inhibitors, including small molecular compounds and small interfering RNA, have been developed and exhibited significantly radiation sensitizing effect [20,21].

Micheliolide (MCL), a natural guaianolide sesquiterpene lactone derivative of parthenolide (PTL) discovered in *Michelia compressa* and *Michelia champaca* plants, has exhibited promising therapeutic efficacy towards inflammation and multiple cancers [22,23]. MCL and PTL both belong to sesquiterpene lactone (SL), which has biological and pharmacological activities, owing to its specific moiety, α -methylene- γ -lactone, which can react with biological nucleophiles, such as cysteine sulfhydryl groups of target proteins [24]. The chemical structure of MCL is shown in Figure 1A. Nuclear factor kappa B (NF- κ B) is well known as a reactive target of SL and its activity was found to be inhibited by SL via preventing the degradation of I κ B- α and I κ B- β [25]. Interestingly, PTL has been shown to radiosensitize prostate cancer cells via inhibiting the NF- κ B pathway [26]. Furthermore, PTL selectively exhibits a radiosensitizing effect on prostate cancer cells, but not normal prostate epithelial cells by activating NADPH oxidase and it mediates intense oxidative stress [27]. However, PTL is unstable under both acidic and alkaline conditions, and this limits its medicinal applications [28]. MCL is more stable than PTL and it can selectively inhibit the growth of acute myelogenous leukemia stem and progenitor cells [29]. Moreover, the dimethylamino Michael adduct of MCL, DMAMCL, is highly promising for the treatment of glioma for crossing the blood-brain barrier, a formidable obstacle for drugs to exert a therapeutic effect in vivo, and it preferentially accumulates in the brain and effectively inhibits glioma cell growth [30]. DMAMCL was recently approved for clinical trials in Australia, owing to the superior oral bioavailability and enhanced therapeutic potential (Trial ID: ACTRN12616000228482). However, the radiosensitizing effect of MCL on NSCLC and the possible underlying mechanisms are still not known.

In the present study, we assessed the radiosensitizing effects of MCL on NSCLC. Our results indicated that MCL sensitized NSCLC, especially p53-deficient cell lines, to radiation under both normoxia and hypoxia via promoting the degradation of HIF-1 α protein. Moreover, we found that p53 played a negative role in the degradation of HIF-1 α that is induced by MCL. These results provide some hints that MCL can be used to sensitize NSCLC to radiotherapy.

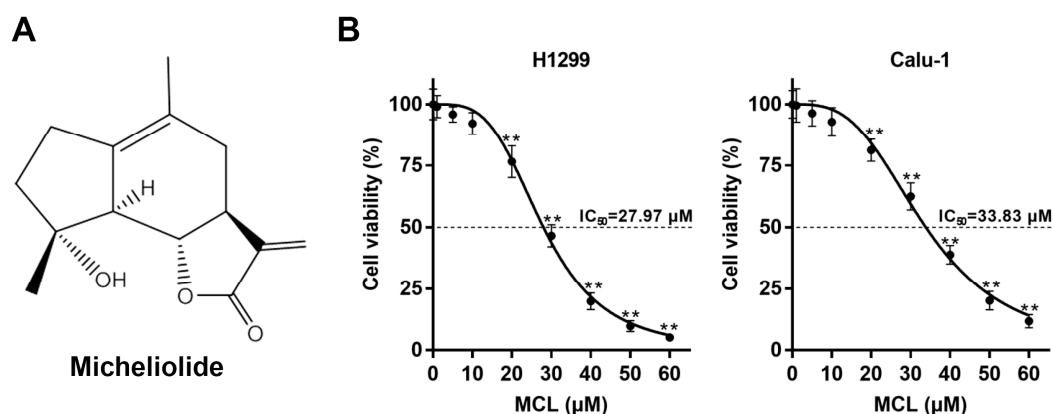


Figure 1. Chemical structure and cytotoxicity of micheliolide (MCL). (A) The chemical structure of MCL. (B) Dose-response curves of MCL for H1299 and Calu-1 cells. **, $p < 0.01$.

2. Results

2.1. MCL Inhibits Cell Growth in NSCLC

We measured the viabilities of H1299 and Calu-1 cells at 24 h after exposure to various concentrations of MCL for 6 h in vitro to evaluate the killing effect of MCL on NSCLC. The cell viabilities of H1299 and Calu-1 cells treated with 5 and 10 μM MCL for 6 h were still higher than 90%, indicating that MCL induced modest cytotoxicity at concentrations less than 20 μM , as shown in Figure 1B. Significant inhibition of cell viability was observed when the cells were treated with relatively high concentrations of MCL (≥ 20 μM) for 6 h. The values of inhibitory concentration at 50% growth (IC_{50}) of MCL for H1299 and Calu-1 cell lines were 27.97 and 33.83 μM , respectively. These results suggest that MCL exerts a cell killing effect in a dose-dependent manner.

2.2. MCL Sensitizes NSCLC to IR under Both Normoxia and Hypoxia

The cell viability of H1299 and Calu-1 cells were determined with CCK-8 after IR with or without MCL treatment to determine whether MCL can sensitize NSCLC to IR. The relative cell viability of H1299 cells decreased to $27.65 \pm 1.80\%$ after 4 Gy of IR with 20 μM MCL treatment, significantly lower than that with IR treatment alone ($69.80 \pm 4.84\%$) or MCL treatment alone ($47.32 \pm 6.01\%$), and the relative cell viability of Calu-1 cells also showed a similar trend, as shown in Figure 2A. Consistently, the enhanced killing effect of MCL was also observed after IR with 8 Gy (Figure 2A). The colony formation assay was further performed to test the radiosensitizing efficiency of MCL in H1299 and Calu-1 cells (Figure 2B). The survival fractions of MCL-pretreated H1299 and Calu-1 cells were significantly lower than their respective controls (no MCL treatment) after exposure to the same IR dose (2–6 Gy). Table 1 showed an increased sensitizer enhancement ratio for Dq (SERDq), 1.62 of H1299 and 1.69 of Calu-1, following MCL treatment.

In general, hypoxia is a tumor microenvironment condition that plays pivotal roles in tumor progression and resistance to radiotherapy [21]. Therefore, we next determine whether MCL exerts a radiosensitizing effect in NSCLC under hypoxic condition. After 4 Gy of radiation under hypoxia, the relative cell viability of H1299 cells decreased to $83.07 \pm 5.85\%$ (Figure 2C), higher than that under normoxia ($69.80 \pm 4.84\%$) (Figure 2A), and the relative cell viability of Calu-1 cells decreased to $84.86 \pm 9.27\%$, which is also higher than that under normoxia ($73.56 \pm 6.14\%$) (Figure 2A). These results

confirmed that NSCLC cells were more resistant to IR under hypoxia than normoxia. Furthermore, after treatment with 4 Gy of radiation plus 20 μ M MCL under hypoxia, the relative cell viability of H1299 cells decreased to $21.84 \pm 1.18\%$, significantly less than that with IR alone ($83.07 \pm 5.85\%$) and MCL treatment alone ($36.41 \pm 4.55\%$), and the relative cell viability of Calu-1 cells decreased to $34.60 \pm 1.14\%$, also significantly less than that with IR alone ($84.86 \pm 9.27\%$) and MCL treatment alone ($50.46 \pm 2.02\%$). A similar trend was also observed after a higher dose of IR (8 Gy) under hypoxia (Figure 2C). These results indicate that MCL sensitizes H1299 and Calu-1 cells to radiation under hypoxia as well as normoxia. Colony formation assay was performed to further confirm the radiosensitizing effect of MCL in NSCLC under hypoxia. Significantly decreased survival fractions of MCL-treated cells were observed compared to controls (irradiated alone) in both H1299 and Calu-1 cells (Figure 2D). The results in Table 2 showed SERDq increased to 2.59 in H1299 and 1.82 in Calu-1 following MCL treatment under hypoxia. In addition, radiosensitization of MCL at a dose of less than 20 μ M was determined with cell viability assay and colony formation assay. Indeed, pretreating H1299 and Calu-1 cells with 5 or 10 μ M MCL sensitized these cells to IR under both normoxia and hypoxia (Figure S1). However, the radiosensitizing effects of MCL at 5 and 10 μ M were weaker than that at 20 μ M (Figure S1, Tables S1 and S2), which indicated that the radiosensitizing effect was affected by MCL in a concentration-dependent manner.

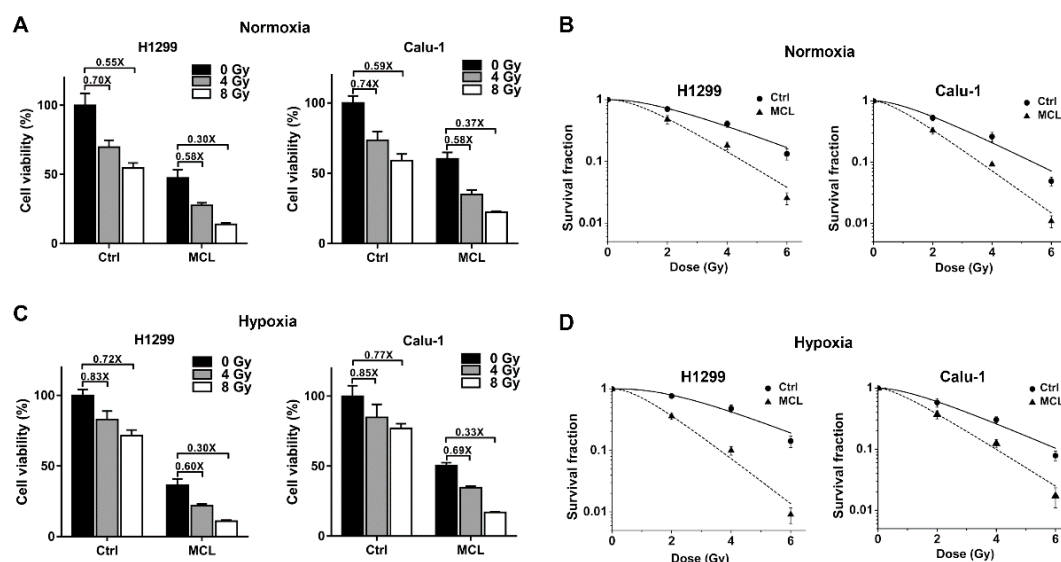


Figure 2. MCL sensitizes H1299 and Calu-1 cells to irradiation (IR). (A) The relative cell viability of H1299 and Calu-1 cells were evaluated at 72 h after IR with or without MCL (20 μ M) pretreatment under normoxia. (B) The survival curves of H1299 and Calu-1 cells after IR with or without MCL pretreatment under normoxia. (C) The relative cell viability of H1299 and Calu-1 cells were evaluated at 72 h after IR with or without MCL (20 μ M) pretreatment under hypoxia. (D) The survival curves of H1299 and Calu-1 cells after IR with or without MCL pretreatment under hypoxia.

Table 1. The survival curve parameters of H1299 and Calu-1 cells after IR with pretreatment of MCL under normoxia.

	H1299			Calu-1		
	SF2	Dq	SERDq	SF2	Dq	SERDq
Ctrl	0.71 ± 0.06	1.95	-	0.53 ± 0.06	1.24	-
MCL	0.48 ± 0.07	1.20	1.62	0.33 ± 0.04	0.73	1.69

SF2, survival fraction at 2 Gy. Dq, quasithreshold dose. SERDq, sensitization enhancement ratio for Dq.

Table 2. The survival curve parameters of H1299 and Calu-1 cells after IR with pretreatment of MCL under hypoxia.

	H1299			Calu-1		
	SF2	Dq	SERDq	SF2	Dq	SERDq
Ctrl	0.77 ± 0.03	2.46	-	0.58 ± 0.09	1.33	-
MCL	0.36 ± 0.04	0.95	2.59	0.37 ± 0.06	0.73	1.82

SF2, survival fraction at 2 Gy. Dq, quasithreshold dose. SERDq, sensitization enhancement ratio for Dq.

Taken together, the aforementioned results suggest MCL exerts a radiosensitizing effect in NSCLC under both normoxia and hypoxia. Moreover, MCL exhibits stronger radiosensitization under hypoxia than that under normoxia.

2.3. MCL Inhibits Radiation- and Hypoxia-Induced HIF-1 α Expression in NSCLC

We first tested whether MCL enhanced radiosensitivity of NSCLC via regulating the NF- κ B pathway to understand the mechanism of radiosensitization of MCL. IR activated the NF- κ B pathway as demonstrated by increased phosphorylation of I κ B α , decreased total I κ B α , and accumulated nuclear localization of NF- κ B p65, as shown in Figure S2. However, the activation of the NF- κ B pathway caused by IR was not affected by pretreatment with MCL, suggesting that NF- κ B pathway might not be involved in the radiosensitizing effect of MCL on NSCLC. Since the HIF-1 α protein is an important negative factor for tumor radiotherapy [31], which is elevated after IR, we next tested whether MCL exerted radiosensitizing effect via inhibiting HIF-1 α pathway. The expression of HIF-1 α was induced higher at 6 h after IR and doses above 4 Gy did not induce further higher HIF-1 α expression in H1299 and Calu-1 cells, as shown in Figure 3A. However, radiation-induced HIF-1 α expression was effectively inhibited with pretreatment of MCL (20 μ M) in H1299 and Calu-1 cells followed by 4 Gy IR (Figure 3B). Furthermore, the results of RT-PCR also revealed that the level of VEGF, a well-known downstream target of HIF-1 α , significantly increased after IR, but this elevated VEGF was also effectively inhibited by MCL treatment (Figure 3C). Meanwhile, the VEGF level was correlated with the HIF-1 α level for the indicated treatments, suggesting that the inhibition of HIF-1 α further downregulated the transcription level of VEGF.

It is known that HIF-1 α is also activated under hypoxia and then activates some downstream genes associated with radioresistance. Hence, we investigated whether MCL could suppress hypoxia-induced HIF-1 α expression in NSCLC. We first focused on the dynamics of intracellular HIF-1 α expression in H1299 and Calu-1 cells under hypoxia. The increase of HIF-1 α protein, especially the posttranslational modification form with higher molecular weight, was observed within 1 h and then reached a peak level around 2 h under hypoxia (Figure 3D). We pretreated H1299 and Calu-1 cells with MCL for 4 h prior to hypoxic culture to evaluate the efficiency of MCL in suppressing hypoxia-induced HIF-1 α expression. MCL pretreatment markedly suppressed hypoxia-induced HIF-1 α expression in both H1299 and Calu-1 cells, as shown in Figure 3E. Consistently, hypoxia-induced VEGF mRNA expression was also significantly reduced following the downregulation of HIF-1 α protein after MCL treatment (Figure 3F). We performed cell viability assay to evaluate the radiosensitizing effect of MCL on H1299 following HIF-1 α knockdown to further confirm that the decrease of HIF-1 α induced by MCL conferred radiosensitization. The cells transfected with siRNA of HIF-1 α showed >90% downregulation of HIF-1 α expression (Figure 3G). Results of cell viability assay showed that MCL pretreatment did not sensitize HIF-1 α knockdown H1299 cells to IR (Figure 3H,I). However, consistent with a previous study [21], siRNA-mediated HIF-1 α downregulation markedly sensitized H1299 cells to IR under both normoxic and hypoxic conditions (Figure 3H,I). These results indicated that MCL sensitizes NSCLC to radiation based on its negative role in HIF-1 α regulation and targeting inhibition of HIF-1 α is an effective approach to reduce radioresistance of NSCLC.

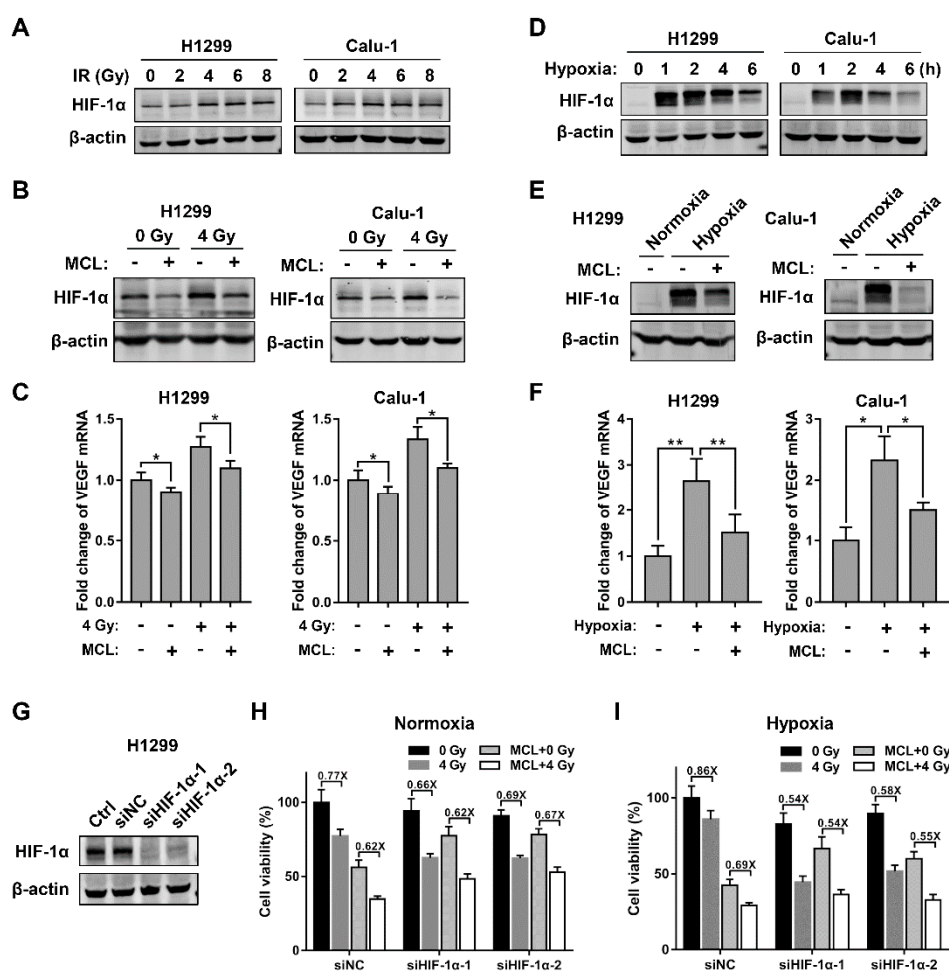


Figure 3. MCL inhibits radiation- and hypoxia-induced HIF-1 α expression. (A) The expression of HIF-1 α protein at 6 h after the indicated doses of IR in H1299 and Calu-1 cells. (B) The expression of HIF-1 α protein at 6 h after the indicated doses of IR in H1299 and Calu-1 cells with or without pretreatment of 20 μ M MCL. (C) The level of 5'-AGGGTCTCGATTGGATGGCA-3' (VEGF) mRNA in indicated cells which were treated in the same way as in (B). *, $p < 0.05$. (D) The expression of HIF-1 α protein at indicated time points after hypoxic exposure in H1299 and Calu-1 cells. (E) The expression of HIF-1 α protein in indicated cells after exposing to hypoxia in the presence or absence of MCL. (F) The level of VEGF mRNA in indicated cells which were treated in the same way as in (E). *, $p < 0.05$; **, $p < 0.01$. (G) Determination of HIF-1 α expression at 48 h after siHIF-1 α transfection in H1299 cells. (H) The relative cell viability of siNC and siHIF-1 α H1299 cells were evaluated at 72 h after IR with or without pretreatment of MCL (20 μ M) under normoxia and hypoxia (I).

2.4. MCL Promotes the Degradation of HIF-1 α

The possible mechanism that could account for decreased MCL-mediated HIF-1 α expression in NSCLC was then studied. The level of HIF-1 α protein was decreased after MCL treatment in a dose-dependent manner in both H1299 and Calu-1 cells. The most significant decrease in HIF-1 α protein level was observed when the concentration of MCL was 20 μ M (Figure 4A). HIF-1 α mRNA expression was detected with RT-PCR after MCL (20 μ M) treatment to verify the possibility that decrease of HIF-1 α protein could be due to inhibited transcription of HIF-1 α gene. However, no changes in HIF-1 α mRNA expression were detected in both H1299 and Calu-1 cells after treated with or without MCL (Figure 4B), which suggested that the loss of HIF-1 α protein in response to MCL treatment did not contribute to the transcriptional regulation. Considering that accelerated protein degradation could also cause the decrease of HIF-1 α protein, we measured the turnover rate of HIF-1 α

protein with cycloheximide (CHX) chase in H1299 and Calu-1 cells pretreated with or without MCL. CHX (100 µg/mL) was used to block total cellular protein synthesis and chase was performed at 2, 5, and 10 min. The decline of HIF-1α protein amount in MCL pretreated cells was faster than that without MCL treatment during the same period, suggesting that MCL accelerated the degradation of HIF-1α protein, as shown in Figure 4C. Since HIF-1α protein was degraded mainly through the ubiquitin-proteasome pathway, we performed immunoprecipitation experiments to detect the level of HIF-1α protein after a proteasome inhibitor (MG132) treatment in MCL-treated H1299 and Calu-1 cells. The inhibition of proteasome with MG132 (20 µM) resulted in the formation of polyubiquitinated HIF-1α, and MCL-treated H1299 and Calu-1 cells led to more polyubiquitinated forms of HIF-1α when compared with cells without MCL treatment (Figure 4D).

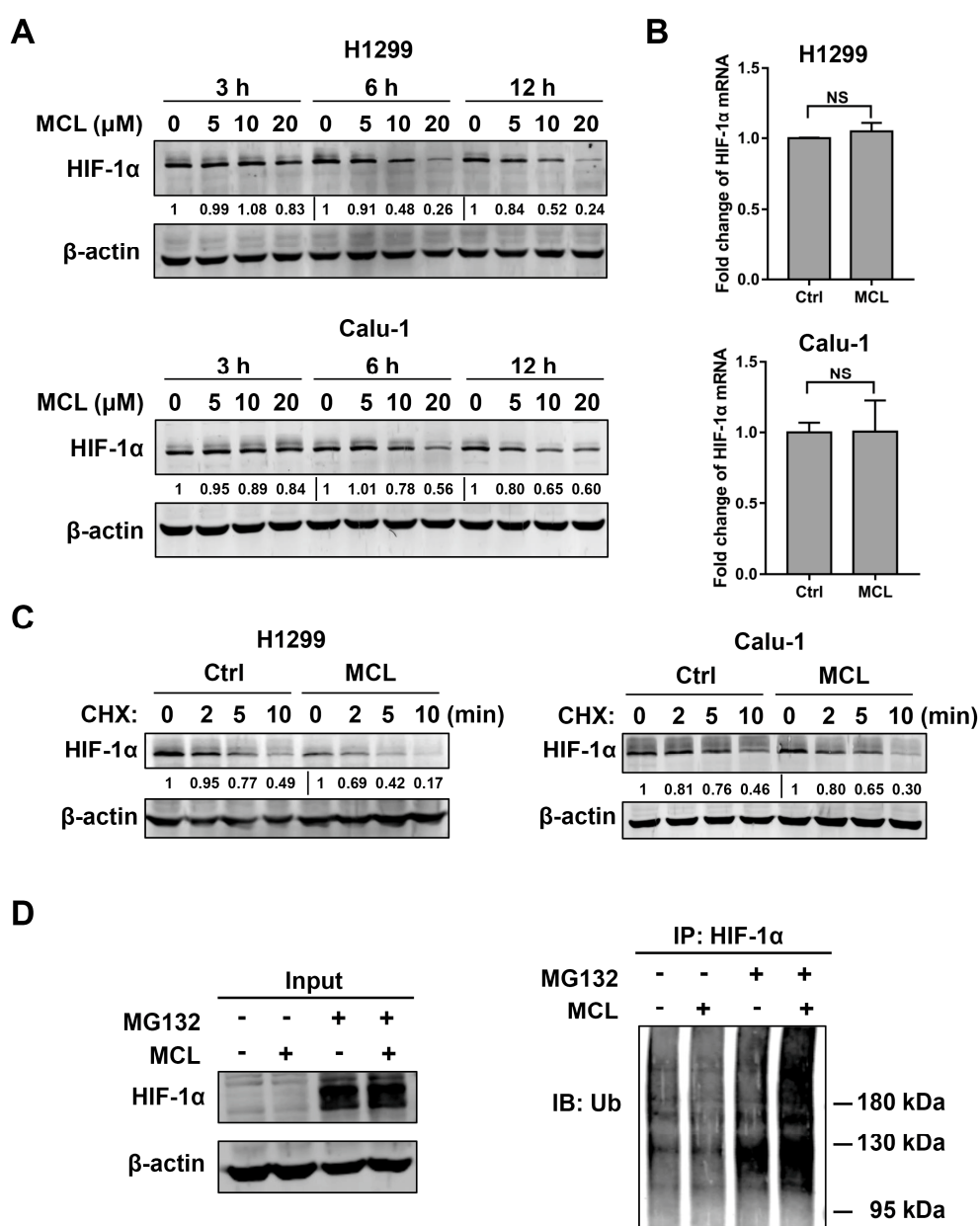


Figure 4. MCL promotes HIF-1α protein degradation in H1299 and Calu-1 cells. (A) The level of HIF-1α protein at indicated time points in H1299 and Calu-1 cells which were treated with various concentrations of MCL. (B) HIF-1α mRNA expression in H1299 and Calu-1 cells after the treatment

of 20 μM MCL for 6 h. NS represents no significance. (C) The level of HIF-1 α protein at indicated time points after cycloheximide (CHX) (100 $\mu\text{g}/\text{mL}$) treatment. Cells were pretreated with 20 μM MCL for 6 h, and then the MCL-containing medium was replaced with medium containing CHX. (D) The ubiquitination level of HIF-1 α in H1299 cells which were treated with a proteasome inhibitor MG132 (20 μM) for 6 h in the presence or absence of 20 μM MCL.

Taken together, these results indicate that MCL treatment can induce the decrease in HIF-1 α protein via promoting its ubiquitin-dependent degradation.

2.5. p53 Attenuates Radiosensitizing Effect of MCL

Interestingly, we found that the sensitizing effect of MCL on H460 (wild-type p53) cells was very weak. The survival fractions of MCL-treated H460 were slightly lower than the control cells after exposure to the same dose IR (2–6 Gy) under both normoxia and hypoxia, and SERDq (Table 3) showed an increase to 1.07 under normoxia and 1.21 under hypoxia in H460 cells, markedly lower than those of p53-null H1299 and Calu-1 cells, as shown in Figure 5A and B. Consistently, no significant decrease in HIF-1 α protein level was observed after MCL treatment in H460 cells (Figure 5C). Furthermore, we assessed the inhibiting capacity of MCL on IR or hypoxia-induced HIF-1 α expression in H460 cells. IR only induced slight expression of HIF-1 α and administering of MCL (20 μM) failed to block the HIF-1 α expression after IR (Figure 5D). Although HIF-1 α expression was greatly induced by hypoxia in H460 cells, MCL treatment did not affect this process (Figure 5E). In addition, MCL also did not affect the induction of VEGF mRNA following IR or hypoxic treatment in H460 cells (Figure 5F). These results provide evidence that p53 might impair MCL-mediated radiosensitization via inhibiting MCL-induced HIF-1 α downregulation.

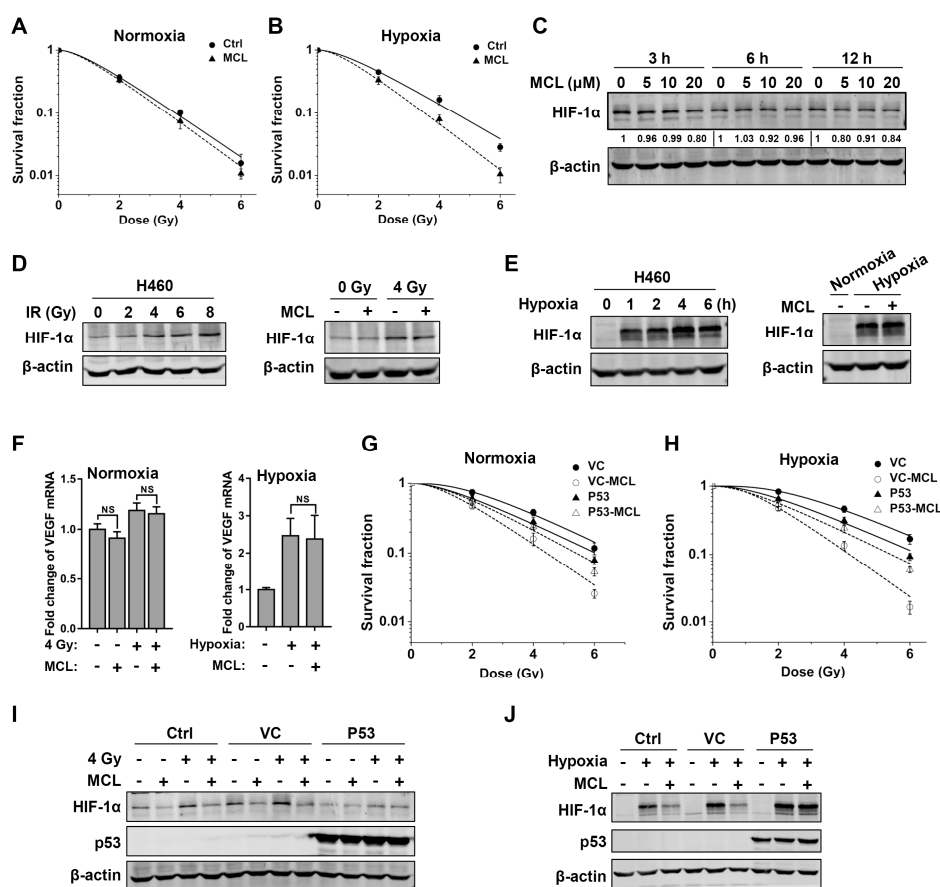


Figure 5. p53 attenuates the radiosensitizing effect of MCL by inhibiting MCL-mediated HIF-1 α protein decline. (A) The survival curves of H460 cells after IR with or without MCL pretreatment under

normoxia and hypoxia (B). (C) The level of HIF-1 α protein at indicated time points in H460 cells after treatment with various concentrations of MCL. (D) The expression of HIF-1 α protein in H460 cells treated with the indicated doses of IR in the presence or absence of 20 μ M MCL. (E) The expression of HIF-1 α protein at indicated time points in H460 cells after exposing to hypoxia in the presence or absence of 20 μ M MCL. (F) The level of VEGF mRNA at 6 h post-IR or at 2 h under hypoxia in the presence or absence of 20 μ M MCL in H460 cells. NS represents no significance. (G) The survival curves of VC and P53 H1299 cells after IR with or without MCL pretreatment under normoxia and hypoxia (H). (I) The effect of MCL pretreatment on the background and radiation-induced HIF-1 α expression in indicated cell lines. (J) The effect of MCL pretreatment on the hypoxia-induced HIF-1 α expression in indicated cell lines.

Table 3. The survival curve parameters of H460 cells after IR with pretreatment of MCL under normoxia and hypoxia.

	Normoxia			Hypoxia		
	SF2	Dq	SERDq	SF2	Dq	SERDq
Ctrl	0.37 \pm 0.04	0.91	-	0.45 \pm 0.02	1.00	-
MCL	0.34 \pm 0.03	0.85	1.07	0.33 \pm 0.05	0.83	1.21

SF2, survival fraction at 2 Gy. Dq, quasithreshold dose. SERDq, sensitization enhancement ratio for Dq.

We engineered stable p53-expressing (P53) as well as the control vector-expressing (VC) H1299 cells and colony formation assay was performed to further confirm the antagonistic action of p53 against radiosensitizing effect of MCL. IR significantly decreased the survival fraction of MCL-treated cells compared to control (irradiated alone) in VC H1299 cells but not in P53 H1299 cells under both normoxic and hypoxic conditions (Figure 5G,H). The survival curve parameters that are presented in Table 4 showed SERDq increased to 1.89 and 2.10 in VC H1299 cells under respective normoxia and hypoxia in the presence of MCL, whereas the SERDq were 1.04 and 1.30 in P53 H1299 cells, indicating the radiosensitizing effect of MCL was markedly inhibited by p53. Consistently, MCL pretreatment effectively inhibited radiation- and hypoxia-induced HIF-1 α expression in control and VC H1299 cells, but the HIF-1 α expression was not affected by MCL treatment in P53 H1299 cells (Figure 5I,J).

Table 4. The survival curve parameters of VC and P53 H1299 cells after IR with pretreatment of MCL under normoxia and hypoxia.

	Normoxia			Hypoxia		
	SF2	Dq	SERDq	SF2	Dq	SERDq
VC	0.74 \pm 0.07	2.24	-	0.83 \pm 0.03	2.78	-
VC-MCL	0.47 \pm 0.03	1.18	1.89	0.47 \pm 0.03	1.33	2.10
P53	0.60 \pm 0.06	1.39	-	0.65 \pm 0.04	1.67	-
P53-MCL	0.56 \pm 0.07	1.33	1.04	0.55 \pm 0.04	1.29	1.30

SF2, survival fraction at 2 Gy. Dq, quasithreshold dose. SERDq, sensitization enhancement ratio for Dq.

Taken together, these findings indicate that p53 strongly impair the radiosensitizing effect of MCL on NSCLC via inhibiting MCL-mediated HIF-1 α decline.

3. Discussion

PTL, a compound with a structure similar to MCL, has been reported to have antitumor activity against NSCLC [32,33]. However, it is unclear whether MCL has antitumor activity against NSCLC cells. In present study, we found that MCL inhibited the growth of NSCLC cells (H1299 and Calu-1) in a concentration-dependent manner. This finding further expanded the antitumor killing spectrum

of MCL. Similar to dimethylaminoparthenolide (DMAPT, a modified form of PTL), MCL also could sensitize NSCLC cells to IR in a concentration-dependent manner (Figure 2 and Figure S1). However, DMAPT sensitized NSCLC to IR by inhibiting NF- κ B activation and blocking DSB repair [34], whereas the activation of the NF- κ B pathway and DSBs repair induced by IR were not affected by MCL in the present study (Figures S2 and S3). In addition, previous studies suggested that cell cycle distribution and ROS production were involved in DMAPT-induced radiosensitization [35,36]. In contrast, MCL treatment did not affect the cell cycle distribution and ROS production after IR in H1299 cells (Figures S4 and S5). Thus, MCL and DMAPT are different in aspects of mechanisms of radiosensitization in NSCLC cells. Moreover, we observed that MCL exhibited higher radiosensitization under hypoxia when compared with normoxia, indicating that MCL also plays a negative regulatory role in hypoxia-induced radioresistance. Our finding suggests MCL combined with radiotherapy has a potential clinical application for attenuating the radioresistance under hypoxia, given that hypoxia is a typical characteristic of solid tumors [37].

Previous works suggested that HIF-1 α is a critical determinant in response to radiotherapy [38,39]. The inhibition of HIF-1 α expression has been regarded as a rational strategy to lower radioresistance of tumors owing to the induction of increased HIF-1 α activity by IR and hypoxia [6,8,20]. In the present study, we also observed that HIF-1 α expression was significantly elevated after IR or hypoxic exposure in both H1299 and Calu-1 cells. In particular, more induction of HIF-1 α protein occurred following hypoxic exposure than IR. Consistently, higher radioresistance under hypoxia in both H1299 and Calu-1 cells confirmed the key role of HIF-1 α in radioresistance. Moreover, our results showed that MCL treatment inhibited both IR- and hypoxia-induced HIF-1 α expression in H1299 and Calu-1 cells. Knocking down HIF-1 α distinctly attenuated the radiosensitization of H1299 cells by MCL, thus confirming that HIF-1 α is a key target for radiosensitization by MCL. Additionally, the IR- and hypoxia-induced VEGF mRNA expression was also inhibited by MCL, reflecting the inhibition of HIF-1 α /VEGF pathway. VEGF, one of the target genes of HIF-1 α , was increased after exposure to IR or hypoxia, and inhibiting VEGF or VEGFR were effective strategies for improving the tumor radiosensitivity in clinical studies [40–42]. Therefore, we speculated inhibition of the HIF-1 α /VEGF pathway might account for the radiosensitizing effect of MCL. This speculation was also supported by another study which suppression of the HIF1- α /VEGF pathway with NVP-BEZ235 or UO126 treatment resulted in the radiosensitization of endometrial cancer cells [43].

It is known that protein expression can be regulated at transcriptional and protein level. In our study, we observed that MCL did not affect the HIF-1 α mRNA expression but decreased HIF-1 α protein, indicating that MCL modulated the expression of HIF-1 α at the protein level. The regulation of HIF-1 α at the protein level is achieved through protein synthesis and degradation. The activation of phosphatidylinositol 3-kinase (PI3K) or mitogen-activated protein kinase (MAPK) pathway was reported to involve in HIF-1 α synthesis [44,45]. In relation, HIF-1 α degradation is regulated primarily via ubiquitin-proteasome system [12]. Moreover, the results of CHX-chase assay indicated that MCL impaired HIF-1 α protein stability via promoting the degradation rate of the HIF-1 α protein. These results were confirmed by our further investigation which showed that ubiquitination level of HIF-1 α was higher in the presence of MCL when compared to that in the absence of MCL after MG132 treatment. Meanwhile, MCL-induced HIF-1 α ubiquitination also suggested that MCL affected HIF-1 α stability in the ubiquitin-proteasome pathway. Recent reports demonstrated that the degradation of HIF-1 α was blocked by histone deacetylases (HDACs), especially HDAC1 and HDAC3, which could bind to oxygen-dependent degradation (ODD) domain of HIF-1 α . In addition, HDAC1 regulates the reduction of the von Hippel-Lindau protein (pVHL), a ubiquitin ligase (E3) protein complex, which mediates the degradation of HIF-1 α [46]. Most notably, PTL can specifically deplete cellular HDAC1 protein [47]. Thus, it is possible that MCL accelerates the process of ubiquitination and proteasomal degradation of HIF-1 α via downregulating HDAC1. Certainly, further studies are needed in order to confirm this speculation. Interestingly, our results showed that no radiosensitization effect of MCL was observed in wild-type p53 cells. Consistently, MCL treatment failed to inhibit

IR- and hypoxia-induced HIF-1 α protein and VEGF mRNA expression in cells with wild-type p53. Our findings suggested that the radiosensitizing effect of MCL was attenuated by p53, owing to failure in HIF-1 α inhibition. When considering the role of p53 in regulating radiosensitizing effect of MCL, the p53 status of individual NSCLC patient should be detected before using MCL as a radiation sensitizer during radiotherapy.

In summary, the present study shows that MCL sensitizes p53-null NSCLC cells to radiotherapy via inhibiting the HIF-1 α expression and its downstream target VEGF. MCL inhibits HIF-1 α expression partly through promoting the ubiquitin-dependent degradation of HIF-1 α protein. However, the presence of p53 could attenuate the radiosensitizing effect of MCL via antagonizing the MCL-mediated HIF-1 α decline (Figure 6). Our results provide support that MCL might be used as a sensitizer to improve the radiotherapy of NSCLC in the future. Certainly, the current results were obtained from experiments *in vitro*. When considering factors, such as bioavailability, distribution, and pharmacokinetics of MCL, might affect its clinical efficacy, the radiosensitizing effect of MCL on NSCLC will be further evaluated *in vivo*.

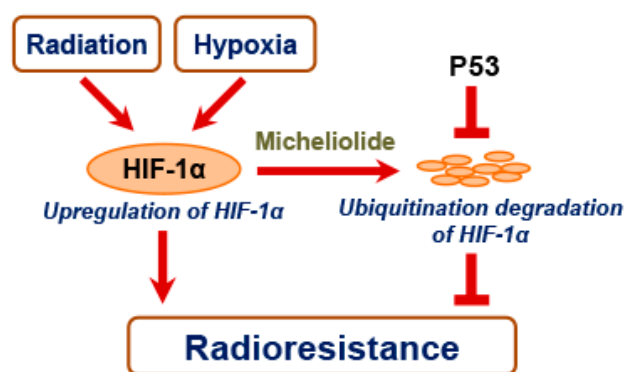


Figure 6. Schematic of MCL sensitizes p53-deficient NSCLC cells to IR via promoting HIF-1 α degradation.

4. Materials and Methods

4.1. Cell Culture and Reagents

The human NSCLC cell lines H1299 (p53-null), Calu-1(p53-null) and H460 (wild-type p53) were purchased from the Cell Bank of Type Culture Collection of Chinese Academy of Sciences (Shanghai, China). The H1299 and Calu-1 cell lines were cultured in RPMI 1640 medium (HyClone; GE Healthcare Life Sciences, Logan, UT, USA) and H460 was cultured in DMEM medium (HyClone), both being supplemented with 10% fetal bovine serum (FBS, HyClone), 100 μ g/mL streptomycin (Gibco, Carlsbad, CA, USA) and 100 U/mL penicillin (Gibco). For normoxic cultures, the cells were maintained at 37 $^{\circ}$ C in a humidified incubator with 5% CO₂ and 95% air. For hypoxic cultures, cells were maintained at 37 $^{\circ}$ C in a Whitley H35 Hypoxystation (Don Whitley Scientific, Shipley, UK) with 1% O₂, 94% N₂ and 5% CO₂. All cell lines were free of mycoplasma. MCL (Wuhan ChemFaces Biochemical, Wuhan, China), protein synthesis inhibitor Cycloheximide (CHX, Sigma, St Louis, MO, USA), and proteasome inhibitor MG132 (Sigma) were dissolved in DMSO.

4.2. Irradiation

The cells were irradiated with a series of doses (0–8 Gy) with an X-ray irradiator (XHA600D, SHINVA, Zibo, China) at a dose rate of 0.189 Gy/min.

4.3. Cell Viability Assay

Cells were treated with MCL (0–60 μ M) for 6 h to assess the cell killing effect of MCL on NSCLC lines. Then the cell viability was measured after pretreatment with MCL (6 h before IR) pulse with IR to assess the radiosensitizing effect of MCL. For hypoxic exposure, four hours after MCL administering,

the cells were moved into hypoxystation for additional 2 h before IR. The MCL-containing medium was replaced with normal culturing medium after IR and then cell viability was evaluated at 72 h after IR. Cell viability was measured with a Cell Counting Kit-8 (CCK-8, ApexBio, Houston, TX, USA). Two hundred microliters of CCK-8 solution was added to each well and incubated for 1 h at 37 °C. Absorbance at 450 nm was measured while using a Microplate Reader (Varioskan Flash, Thermo Fisher, Waltham, MA, USA). IC50 determination was performed using GraphPad Prism 7.0 software (GraphPad Prism Software, Inc., San Diego, CA, USA).

4.4. Colony Formation Assay

The cells were plated into 35 mm culture dishes at a density of 200 to 5000 cells/dish. After attaching on the surface of dishes, the cells were treated with MCL and radiation subsequently. The cells were treated with MCL for 6 h prior to radiation exposure. For hypoxic exposure, four hours after MCL administering, the cells were moved into hypoxystation for additional 2 h before IR. After IR, the MCL-containing medium was replaced with normal culturing medium and the cells were maintained under normoxic conditions. Eight to twelve days later, the cells were washed and then stained with 1% crystal violet, and the colonies containing ≥ 50 cells were counted. Plating efficiency (PE) was calculated by dividing the average number of colonies per dish by the number of cells seeded. The survival fraction (SF) was calculated by normalization to the PE of appropriate control groups. Survival curves were constructed with Origin 8.0 software (OriginLab, Northampton, MA, USA). The survival curve parameters, D0 and Dq, were calculated by fitting the data with the single-hit multi-target model [48].

4.5. Western Blot and Immunoprecipitation

Whole-cell protein was extracted with RIPA lysis buffer (Beyotime Biotechnology, Shanghai, China) and the protein concentration was determined with a BCA protein assay kit (Beyotime Biotechnology). The proteins were then separated with 6%–12% sodium dodecyl sulfate-polyacrylamide gel electrophoresis (SDS-PAGE) and then transferred to polyvinylidene fluoride membranes (Merck Millipore, Darmstadt, Germany). The membranes were blocked in 5% skim milk (BD/Difco, Sparks, MD, USA) for 1 h, and then incubated with different primary antibodies at 4 °C overnight. The primary antibodies utilized were: anti-HIF-1 α (1:1000, Protein Tech Group, Wuhan, China), anti-ubiquitin (1:1000, Cell Signaling Technology, Beverly, MA, USA), anti- γ -H2AX (phospho S139) (1:1000, Abcam, Cambridge, UK), anti-I κ B α (1:1000, Cell Signaling Technology), anti-phospho-I κ B α (Ser32/36) (1:1000, Cell Signaling Technology), or anti- β -actin (1:1000, Protein Tech Group). After extensive washing with TBST, blots were incubated with IRDye-conjugated secondary antibodies (1:10000, Li-COR Biosciences, Lincoln, NE, USA) for 1 h at room temperature. Images of immunoreactive bands were captured with Odyssey CLx Infrared Imaging system (Li-COR Biosciences).

For immunoprecipitation (IP), 2 g of anti-HIF-1 α (Abcam) incubated with 4 mg of cell lysate, followed by capturing with protein-A/G agarose (Beyotime Biotechnology). The beads were washed extensively and then suspended in SDS loading buffer for western blot analysis.

4.6. RT-PCR

RT-PCR was performed with One Step SYBR[®] PrimeScript[™] RT-PCR Kits (Takara Bio, Dalian, China) on a Roche 480 Light Cycler (Roche, Basel, Switzerland). The primers used for PCR amplification are shown as follows: 5'-GAACGTCGAAAAGAAAAGTCTCG-3', 5'-CC TTATCAAGATGCGAACTACA-3' (HIF-1 α); 5'-AGGGCAGAATCATCACGAAGT-3', 5'-AGGG TCTCGATTGGATGGCA-3' (VEGF); and, 5'-CTGGGACGACATGGAGAAA-3', 5'-AAGGAA GGCTGGAAGAGTGC-3' (ACTB). ACTB was used as a normalizing control and data analysis was performed as previously described [49], through calculating fold changes by the $2^{-\Delta\Delta C_t}$ method.

4.7. Small Interfering RNA Transfection

The transfection of cells with negative control RNA sequence (siNC) or HIF-1 α small interfering RNA (siHIF-1 α ; GenePharma, Shanghai, China) were carried out with Lipofectamine 2000 Transfection Reagent (Invitrogen, Carlsbad, CA, USA) according to the manufacturer's instructions. The target sequences of siHIF-1 α are as follows: siHIF-1 α -1: GGGTAAAGAACAAAACACA; siHIF-1 α -2: AACTAACTGGACACAGTGTGT. Forty-eight hours after siNC and siHIF-1 α transfection, the cells were used for the further experiment.

4.8. Retroviral Infection

The p53 overexpressed plasmid was generated by subcloning human full length TP53 cDNA (NM_000017.11) into the pCDH-CMV-MCS-EF1-Puro lentiviral plasmid. Lentiviruses were prepared through co-transfecting HEK293T cells with the P53 overexpressed plasmid and the packaging plasmids (psPAX2 and pMD2.G), as described previously [50]. The H1299 cells were infected with lentiviruses and the stable cell lines expressing p53 were selected for 10 days with puromycin (2 μ g/mL) from 48 h after infection.

4.9. Statistical Analysis

All of the experiments were performed at least three times. The data were presented as mean \pm SD. Differences were assessed using Student's t test with SPSS v17.0 software (SPSS, Chicago, IL, USA), and cases with $p < 0.05$ was considered to be a statistically significant difference.

Supplementary Materials: The following are available online at <http://www.mdpi.com/1422-0067/21/9/3392/s1>.

Author Contributions: Conceptualization, P.K., G.C. and W.H.; methodology, P.K., M.Y., W.A.A., L.N. and G.C.; software, P.K.; validation, P.K., K.N.Y., G.C. and W.H.; formal analysis, P.K.; investigation, P.K.; resources, P.K.; data curation, P.K. and L.N.; writing—original draft preparation, P.K. and G.C.; writing—review and editing, K.N.Y. and W.H.; visualization, P.K.; supervision, G.C. and W.H.; project administration, G.C. and W.H.; funding acquisition, G.C. and W.H. All authors have read and agreed to the published version of the manuscript.

Funding: This research was supported by the Chinese National Natural Science Foundation (grant nos. 81703168, U1632145 and 81227902), the Natural Science Fund of Anhui Province (1608085QH181), Key Program of 13th five-year plan, CASHIPS, Grant No. KP-2017-25, CASHIPS Director's Fund (grant no.YZJJ2018QN19) and project funded by the Priority Academic Program Development of Jiangsu Higher Education Institutions (PAPD) and Jiangsu Provincial Key Laboratory of Radiation Medicine and Protection. This research was also supported by the research grant IRF/0024 from the State Key Laboratory in Marine Pollution, City University of Hong Kong.

Conflicts of Interest: The authors declare no conflict of interest.

Abbreviations

IR	Irradiation
MCL	Micheliolide
PTL	Parthenolide
DMAMCL	Dimethylamino Michael adduct of MCL
NSCLC	Non-small-cell lung cancer
IC50	Inhibitory concentration at 50% growth
DSB	DNA double-strand break
HIF-1 α	Hypoxia-inducible factor-1 α
VEGF	Vascular endothelial growth factor
CHX	Cycloheximide
SF2	Survival fraction at 2 Gy
Dq	Quasithreshold dose
SERDq	Sensitizer enhancement ratio for Dq
NF- κ B	Nuclear factor kappa B
HDAC	Histone deacetylase

References

1. Bray, F.; Ferlay, J.; Soerjomataram, I.; Siegel, R.L.; Torre, L.A.; Jemal, A. Global cancer statistics 2018: GLOBOCAN estimates of incidence and mortality worldwide for 36 cancers in 185 countries. *CA Cancer J. Clin.* **2018**, *68*, 394–424. [[CrossRef](#)] [[PubMed](#)]
2. Meza, R.; Meernik, C.; Jeon, J.; Cote, M.L. Lung cancer incidence trends by gender, race and histology in the United States, 1973–2010. *PLoS ONE* **2015**, *10*, e0121323. [[CrossRef](#)] [[PubMed](#)]
3. Baumann, M.; Stamatis, G.; Thomas, M. Therapy of localized non-small cell lung cancer (take home messages). *Lung Cancer* **2001**, *33*, S47–S49. [[CrossRef](#)]
4. Bristow, R.G.; Alexander, B.; Baumann, M.; Bratman, S.V.; Brown, J.M.; Camphausen, K.; Choyke, P.; Citrin, D.; Contessa, J.N.; Dicker, A. Combining precision radiotherapy with molecular targeting and immunomodulatory agents: a guideline by the American Society for Radiation Oncology. *Lancet Oncol.* **2018**, *19*, e240–e251. [[CrossRef](#)]
5. Brown, J.M.; Wilson, W.R. Exploiting tumour hypoxia in cancer treatment. *Nat. Rev. Cancer* **2004**, *4*, 437. [[CrossRef](#)] [[PubMed](#)]
6. Moeller, B.; Dewhirst, M. HIF-1 and tumour radiosensitivity. *Br. J. Cancer* **2006**, *95*, 1. [[CrossRef](#)]
7. Wang, G.L.; Jiang, B.-H.; Rue, E.A.; Semenza, G.L. Hypoxia-inducible factor 1 is a basic-helix-loop-helix-PAS heterodimer regulated by cellular O₂ tension. *Proc. Natl. Acad. Sci. USA* **1995**, *92*, 5510–5514. [[CrossRef](#)]
8. Ivan, M.; Kondo, K.; Yang, H.; Kim, W.; Valiando, J.; Ohh, M.; Salic, A.; Asara, J.M.; Lane, W.S.; Kaelin, W.G., Jr. HIF α targeted for VHL-mediated destruction by proline hydroxylation: implications for O₂ sensing. *Science* **2001**, *292*, 464–468. [[CrossRef](#)]
9. Berra, E.; Roux, D.; Richard, D.E.; Pouyssegur, J. Hypoxia-inducible factor-1 α (HIF-1 α) escapes O₂-driven proteasomal degradation irrespective of its subcellular localization: nucleus or cytoplasm. *EMBO Rep.* **2001**, *2*, 615–620. [[CrossRef](#)]
10. Harris, A.L. Hypoxia—a key regulatory factor in tumour growth. *Nat. Rev. Cancer* **2002**, *2*, 38. [[CrossRef](#)]
11. Brunelle, J.K.; Bell, E.L.; Quesada, N.M.; Vercauteren, K.; Tiranti, V.; Zeviani, M.; Scarpulla, R.C.; Chandel, N.S. Oxygen sensing requires mitochondrial ROS but not oxidative phosphorylation. *Cell Metab.* **2005**, *1*, 409–414. [[CrossRef](#)]
12. Semenza, G.L. Targeting HIF-1 for cancer therapy. *Nat. Rev. Cancer* **2003**, *3*, 721. [[CrossRef](#)]
13. Kim, W.-Y.; Oh, S.H.; Woo, J.-K.; Hong, W.K.; Lee, H.-Y. Targeting heat shock protein 90 overrides the resistance of lung cancer cells by blocking radiation-induced stabilization of hypoxia-inducible factor-1 α . *Cancer Res.* **2009**, *69*, 1624–1632. [[CrossRef](#)]
14. Pidgeon, G.P.; Barr, M.P.; Harmey, J.H.; Foley, D.A.; Bouchier-Hayes, D.J. Vascular endothelial growth factor (VEGF) upregulates BCL-2 and inhibits apoptosis in human and murine mammary adenocarcinoma cells. *Br. J. Cancer* **2001**, *85*, 273. [[CrossRef](#)] [[PubMed](#)]
15. Calvaruso, M.; Pucci, G.; Musso, R.; Bravata, V. Nutraceutical Compounds as Sensitizers for Cancer Treatment in Radiation Therapy. *Int. J. Mol. Sci.* **2019**, *20*, 5267. [[CrossRef](#)] [[PubMed](#)]
16. Baker, L.; Boulton, J.; Walker-Samuel, S.; Chung, Y.; Jamin, Y.; Ashcroft, M.; Robinson, S. The HIF-pathway inhibitor NSC-134754 induces metabolic changes and anti-tumour activity while maintaining vascular function. *Br. J. Cancer* **2012**, *106*, 1638. [[CrossRef](#)] [[PubMed](#)]
17. Aebbersold, D.M.; Burri, P.; Beer, K.T.; Laissue, J.; Djonov, V.; Greiner, R.H.; Semenza, G.L. Expression of hypoxia-inducible factor-1 α : a novel predictive and prognostic parameter in the radiotherapy of oropharyngeal cancer. *Cancer Res.* **2001**, *61*, 2911–2916.
18. Koukourakis, M.I.; Giatromanolaki, A.; Skarlatos, J.; Corti, L.; Blandamura, S.; Piazza, M.; Gatter, K.C.; Harris, A.L. Hypoxia inducible factor (HIF-1 α and HIF-2 α) expression in early esophageal cancer and response to photodynamic therapy and radiotherapy. *Cancer Res.* **2001**, *61*, 1830–1832.
19. Hui, E.P.; Chan, A.T.; Pezzella, F.; Turley, H.; To, K.-F.; Poon, T.C.; Zee, B.; Mo, F.; Teo, P.M.; Huang, D.P. Coexpression of hypoxia-inducible factors 1 α and 2 α , carbonic anhydrase IX, and vascular endothelial growth factor in nasopharyngeal carcinoma and relationship to survival. *Clin. Cancer Res.* **2002**, *8*, 2595–2604.
20. Moeller, B.J.; Cao, Y.; Li, C.Y.; Dewhirst, M.W. Radiation activates HIF-1 to regulate vascular radiosensitivity in tumors: role of reoxygenation, free radicals, and stress granules. *Cancer Cell* **2004**, *5*, 429–441. [[CrossRef](#)]
21. Zhang, X.; Kon, T.; Wang, H.; Li, F.; Huang, Q.; Rabbani, Z.N.; Kirkpatrick, J.P.; Vujaskovic, Z.; Dewhirst, M.W.; Li, C.-Y. Enhancement of hypoxia-induced tumor cell death in vitro and radiation therapy in vivo by use of

- small interfering RNA targeted to hypoxia-inducible factor-1 α . *Cancer Res.* **2004**, *64*, 8139–8142. [[CrossRef](#)] [[PubMed](#)]
22. Viennois, E.; Xiao, B.; Ayyadurai, S.; Wang, L.; Wang, P.G.; Zhang, Q.; Chen, Y.; Merlin, D. Micheliolide, a new sesquiterpene lactone that inhibits intestinal inflammation and colitis-associated cancer. *Lab. Invest.* **2014**, *94*, 950. [[CrossRef](#)] [[PubMed](#)]
 23. Li, J.; Li, S.; Guo, J.; Li, Q.; Long, J.; Ma, C.; Ding, Y.; Yan, C.; Li, L.; Wu, Z. Natural product micheliolide (MCL) irreversibly activates pyruvate kinase M2 and suppresses leukemia. *J. Med. Chem.* **2018**, *61*, 4155–4164. [[CrossRef](#)] [[PubMed](#)]
 24. Ghantous, A.; Gali-Muhtasib, H.; Vuorela, H.; Saliba, N.A.; Darwiche, N. What made sesquiterpene lactones reach cancer clinical trials? *Drug Discov. Today* **2010**, *15*, 668–678. [[CrossRef](#)]
 25. Hehner, S.P.; Heinrich, M.; Bork, P.M.; Vogt, M.; Ratter, F.; Lehmann, V.; Schulze-Osthoff, K.; Dröge, W.; Schmitz, M.L. Sesquiterpene lactones specifically inhibit activation of NF- κ B by preventing the degradation of I κ B- α and I κ B- β . *J. Biol. Chem.* **1998**, *273*, 1288–1297. [[CrossRef](#)]
 26. Sun, Y.; Clair, D.K.S.; Fang, F.; Warren, G.W.; Rangnekar, V.M.; Crooks, P.A.; Clair, W.H.S. The radiosensitization effect of parthenolide in prostate cancer cells is mediated by nuclear factor- κ B inhibition and enhanced by the presence of PTEN. *Mol. Cancer Ther.* **2007**, *6*, 2477–2486. [[CrossRef](#)]
 27. Sun, Y.; Clair, D.K.S.; Xu, Y.; Crooks, P.A.; Clair, W.H.S. A NADPH oxidase-dependent redox signaling pathway mediates the selective radiosensitization effect of parthenolide in prostate cancer cells. *Cancer Res.* **2010**, *70*, 2880–2890. [[CrossRef](#)]
 28. Jin, P.; Madieh, S.; Augsburger, L.L. The solution and solid state stability and excipient compatibility of parthenolide in feverfew. *AAPS PharmSciTech* **2007**, *8*, 200. [[CrossRef](#)]
 29. Zhang, Q.; Lu, Y.; Ding, Y.; Zhai, J.; Ji, Q.; Ma, W.; Yang, M.; Fan, H.; Long, J.; Tong, Z. Guaianolide sesquiterpene lactones, a source to discover agents that selectively inhibit acute myelogenous leukemia stem and progenitor cells. *J. Med. Chem.* **2012**, *55*, 8757–8769. [[CrossRef](#)]
 30. An, Y.; Guo, W.; Li, L.; Xu, C.; Yang, D.; Wang, S.; Lu, Y.; Zhang, Q.; Zhai, J.; Fan, H.; et al. Micheliolide derivative DMAMCL inhibits glioma cell growth in vitro and in vivo. *PLoS ONE* **2015**, *10*, e0116202. [[CrossRef](#)]
 31. Unruh, A.; Ressel, A.; Mohamed, H.G.; Johnson, R.S.; Nadrowitz, R.; Richter, E.; Katschinski, D.M.; Wenger, R.H. The hypoxia-inducible factor-1 α is a negative factor for tumor therapy. *Oncogene* **2003**, *22*, 3213. [[CrossRef](#)] [[PubMed](#)]
 32. Zhao, X.; Liu, X.; Su, L. Parthenolide induces apoptosis via TNFRSF10B and PMAIP1 pathways in human lung cancer cells. *J. Exp. Clin. Cancer Res.* **2014**, *33*, 3. [[CrossRef](#)] [[PubMed](#)]
 33. Zhang, D.; Qiu, L.; Jin, X.; Guo, Z.; Guo, C. Nuclear factor-kappaB inhibition by parthenolide potentiates the efficacy of Taxol in non-small cell lung cancer in vitro and in vivo. *Mol. Cancer Res.* **2009**, *7*, 1139–1149. [[CrossRef](#)] [[PubMed](#)]
 34. Deraska, P.V.; O’Leary, C.; Reavis, H.D.; Labe, S.; Dinh, T.K.; Lazaro, J.B.; Sweeney, C.; D’Andrea, A.D. NF-kappaB inhibition by dimethylaminoparthenolide radiosensitizes non-small-cell lung carcinoma by blocking DNA double-strand break repair. *Cell Death Discov.* **2018**, *4*, 10. [[CrossRef](#)]
 35. Estabrook, N.C.; Chin-Sinex, H.; Borgmann, A.J.; Dhaemers, R.M.; Shapiro, R.H.; Gilley, D.; Huda, N.; Crooks, P.; Sweeney, C.; Mendonca, M.S. Inhibition of NF-kappaB and DNA double-strand break repair by DMAPT sensitizes non-small-cell lung cancers to X-rays. *Free Radic. Biol. Med.* **2011**, *51*, 2249–2258. [[CrossRef](#)]
 36. Shanmugam, R.; Kusumanchi, P.; Appaiah, H.; Cheng, L.; Crooks, P.; Neelakantan, S.; Peat, T.; Klaunig, J.; Matthews, W.; Nakshatri, H.; et al. A water soluble parthenolide analog suppresses in vivo tumor growth of two tobacco-associated cancers, lung and bladder cancer, by targeting NF-kappaB and generating reactive oxygen species. *Int. J. Cancer* **2011**, *128*, 2481–2494. [[CrossRef](#)]
 37. Ackerman, D.; Simon, M.C. Hypoxia, lipids, and cancer: Surviving the harsh tumor microenvironment. *Trends Cell Biol.* **2014**, *24*, 472–478. [[CrossRef](#)]
 38. Koukourakis, M.I.; Giatromanolaki, A.; Sivridis, E.; Simopoulos, C.; Turley, H.; Talks, K.; Gatter, K.C.; Harris, A.L.; Tumour and Angiogenesis Research Group. Hypoxia-inducible factor (HIF1A and HIF2A), angiogenesis, and chemoradiotherapy outcome of squamous cell head-and-neck cancer. *Int. J. Radiat. Oncol.* **2002**, *53*, 1192–1202. [[CrossRef](#)]

39. Bachtary, B.; Schindl, M.; Pötter, R.; Dreier, B.; Knocke, T.H.; Hainfellner, J.A.; Horvat, R.; Birner, P. Overexpression of hypoxia-inducible factor 1 α indicates diminished response to radiotherapy and unfavorable prognosis in patients receiving radical radiotherapy for cervical cancer. *Clin. Cancer Res.* **2003**, *9*, 2234–2240.
40. Gorski, D.H.; Beckett, M.A.; Jaskowiak, N.T.; Calvin, D.P.; Mauceri, H.J.; Salloum, R.M.; Seetharam, S.; Koons, A.; Hari, D.M.; Kufe, D.W. Blockade of the vascular endothelial growth factor stress response increases the antitumor effects of ionizing radiation. *Cancer Res.* **1999**, *59*, 3374–3378.
41. Lee, C.-G.; Heijn, M.; di Tomaso, E.; Griffon-Etienne, G.; Ancukiewicz, M.; Koike, C.; Park, K.; Ferrara, N.; Jain, R.K.; Suit, H.D. Anti-vascular endothelial growth factor treatment augments tumor radiation response under normoxic or hypoxic conditions. *Cancer Res.* **2000**, *60*, 5565–5570. [[PubMed](#)]
42. Hess, C.; Vuong, V.; Hegyi, I.; Riesterer, O.; Wood, J.; Fabbro, D.; Glanzmann, C.; Bodis, S.; Pruschy, M. Effect of VEGF receptor inhibitor PTK787/ZK222548 combined with ionizing radiation on endothelial cells and tumour growth. *Br. J. Cancer* **2001**, *85*, 2010. [[CrossRef](#)] [[PubMed](#)]
43. Miyasaka, A.; Oda, K.; Ikeda, Y.; Sone, K.; Fukuda, T.; Inaba, K.; Makii, C.; Enomoto, A.; Hosoya, N.; Tanikawa, M. PI3K/mTOR pathway inhibition overcomes radioresistance via suppression of the HIF1- α /VEGF pathway in endometrial cancer. *Gynecol. Oncol.* **2015**, *138*, 174–180. [[CrossRef](#)] [[PubMed](#)]
44. Zhong, H.; Chiles, K.; Feldser, D.; Laughner, E.; Hanrahan, C.; Georgescu, M.; Simons, J.; Semenza, G. Modulation of HIF-1 α expression by the epidermal growth factor/phosphatidylinositol 3-kinase/PTEN/AKT/FRAP pathway in human prostate cancer cells: implications for tumor angiogenesis and therapeutics. *Cancer Res.* **2000**, *60*, 1541–1545.
45. Fukuda, R.; Hirota, K.; Fan, F.; Do Jung, Y.; Ellis, L.M.; Semenza, G.L. Insulin-like growth factor 1 induces hypoxia-inducible factor 1-mediated vascular endothelial growth factor expression, which is dependent on MAP kinase and phosphatidylinositol 3-kinase signaling in colon cancer cells. *J. Biol. Chem.* **2002**, *277*, 38205–38211. [[CrossRef](#)]
46. Kim, S.-H.; Jeong, J.-W.; Park, J.; Lee, J.-W.; Seo, J.H.; Jung, B.-K.; Bae, M.-K.; Kim, K.-W. Regulation of the HIF-1 α stability by histone deacetylases. *Oncol. Rep.* **2007**, *17*, 647–651. [[CrossRef](#)]
47. Gopal, Y.V.; Arora, T.S.; Van Dyke, M.W. Parthenolide specifically depletes histone deacetylase 1 protein and induces cell death through ataxia telangiectasia mutated. *Chem. Biol.* **2007**, *14*, 813–823. [[CrossRef](#)]
48. Franken, N.A.; Rodermond, H.M.; Stap, J.; Haveman, J.; Van Bree, C. Clonogenic assay of cells in vitro. *Nat. Protoc.* **2006**, *1*, 2315. [[CrossRef](#)]
49. Livak, K.J.; Schmittgen, T.D. Analysis of relative gene expression data using real-time quantitative PCR and the 2- $\Delta\Delta$ CT method. *Methods* **2001**, *25*, 402–408. [[CrossRef](#)]
50. Zhu, S.; Wang, H.; Ding, S. Reprogramming fibroblasts toward cardiomyocytes, neural stem cells and hepatocytes by cell activation and signaling-directed lineage conversion. *Nat. Protoc.* **2015**, *10*, 959. [[CrossRef](#)]

